
Figures and figure supplements

Defining cellular population dynamics at single-cell resolution during prostate cancer progression

Alexandre A Germanos *et al.*

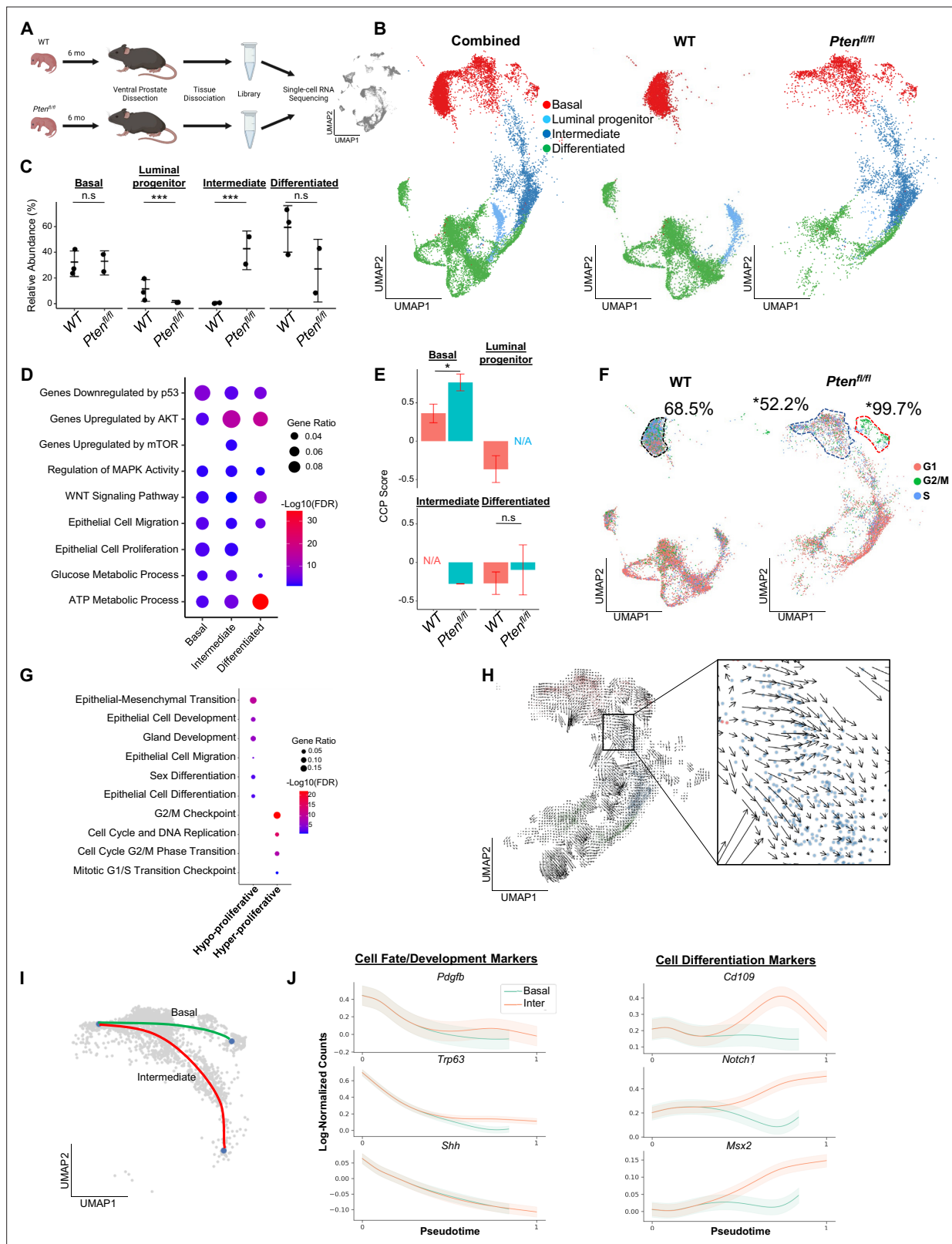


Figure 1. Proliferative split in basal cancer cells enables expansion of intermediate cells. **(A)** Simplified schematic of single-cell RNA sequencing of WT and *Pten^{fl/fl}* ventral prostates. **(B)** UMAP of WT and *Pten^{fl/fl}* epithelial cells. Left, both conditions superposed; middle, WT only; right, *Pten^{fl/fl}* only. Epithelial cell types are demarcated by color (red = basal, light blue = luminal progenitor, dark blue = intermediate, green = differentiated). **(C)** Relative abundance of epithelial cells in WT (n=3) and *Pten^{fl/fl}* (n=2) mice. Y-axis shows the % composition of each sample by cell type (***)p<0.001, negative

Figure 1 continued on next page

Figure 1 continued

binomial test). Data presented as +/-SD. **(D)** Top GSEA results enriched in *Pten*^{fl/fl} compared to WT for each epithelial subtype. Intermediate cells in *Pten*^{fl/fl} were compared to luminal progenitor cells in WT. All pathways are enriched with FDR <0.05. **(E)** Proliferation signature (CCP) composite score in epithelial cells, clustered by condition (Data presented as +/-SD, *p<0.05, n.s.=not significant, permutation test). N/A indicates missing data due to no cells being present in the condition. WT n=3, *Pten*^{fl/fl} n=2. **(F)** UMAP visualization of cell cycle phase assignment per cell, showing % cells in non-G1 (S or G2/M) (black border = WT basal cells, blue border = hypo-proliferative basal cells in *Pten*^{fl/fl}, and red border = hyper-proliferative basal cells in *Pten*^{fl/fl}. *p<0.05, chi-square test). **(G)** GSEA between hyper- and hypo-proliferative basal clusters in *Pten*^{fl/fl}. All pathways are enriched with FDR <0.05. **(H)** RNA velocity analysis of *Pten*^{fl/fl} epithelial cells; highlighted section shows intersection of basal and intermediate cells. **(I)** Pseudotime trajectories drawn by Palantir through the basal and intermediate compartments, with hypo-proliferating basal cells as the designated start point. **(J)** Expression of important cell fate and differentiation regulators along basal-intermediate trajectory.

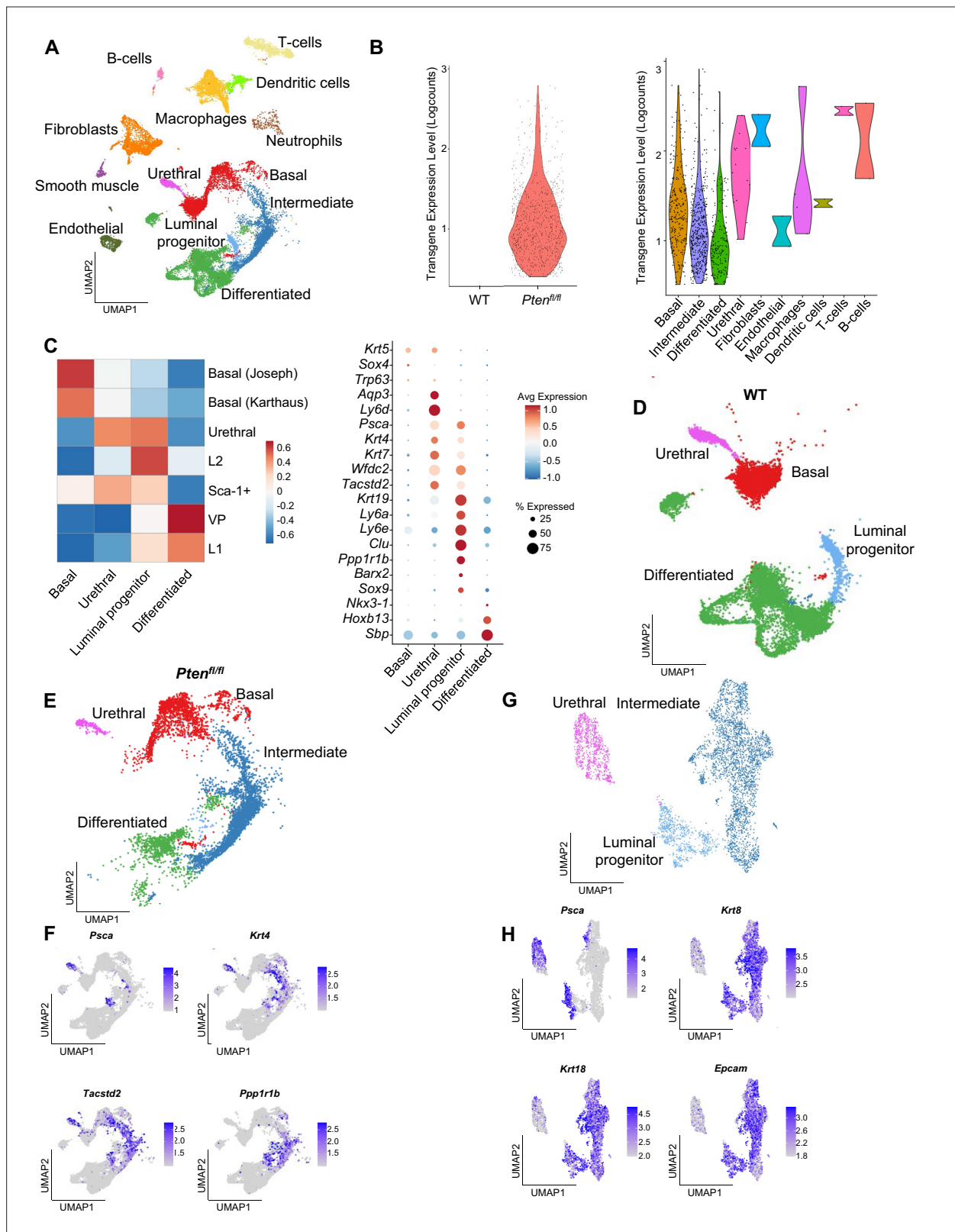


Figure 1—figure supplement 1. Epithelial cells contain published subtypes and urethral cells. **(A)** UMAP visualization of all cells in WT and *Pten*^{fl/fl} ventral prostates, colored and labeled by cell ID. **(B)** Violin plots of *rTA-eGFP* transgene expression. Left, transgene expression in WT and *Pten*^{fl/fl} mice. Right, expression in *Pten*^{fl/fl} cell types. **(C)** Heatmap of composite scores of published prostate epithelial subtype signatures in basal, urethral, luminal progenitor, and differentiated cells in WT mice (left). Dot plot of epithelial biomarker gene expression in WT mice (right). **(D)** UMAP visualization of WT ventral prostate cells, colored by cell ID. **(E)** UMAP visualization of *Pten*^{fl/fl} ventral prostate cells, colored by cell ID. **(F)** UMAP visualization of *Pten*^{fl/fl} ventral prostate cells, colored by expression of *PscA*, *Krt4*, *Tacstd2*, and *Ppp1r1b*. **(G)** UMAP visualization of *Pten*^{fl/fl} ventral prostate cells, colored by expression of *PscA*, *Krt8*, *Krt18*, and *Epcam*. **(H)** UMAP visualization of *Pten*^{fl/fl} ventral prostate cells, colored by expression of *PscA*, *Krt8*, *Krt18*, and *Epcam*.

Figure 1—figure supplement 1 continued on next page

Figure 1—figure supplement 1 continued

of epithelial cells in WT prostates, colored and labeled by cell ID. **(E)** UMAP visualization of epithelial cells in *Pten*^{fl/fl} prostates, colored and labeled by cell ID. **(F)** UMAP visualization of published intermediate cell biomarkers in WT and *Pten*^{fl/fl} mice. **(G)** UMAP visualization of urethral, luminal progenitor, and intermediate cells in WT and *Pten*^{fl/fl} mice, colored and labeled by cell ID. **(H)** UMAP visualization of *Psca*, pan-epithelial and luminal biomarkers in urethral, luminal progenitor, and intermediate cells in WT and *Pten*^{fl/fl} mice.

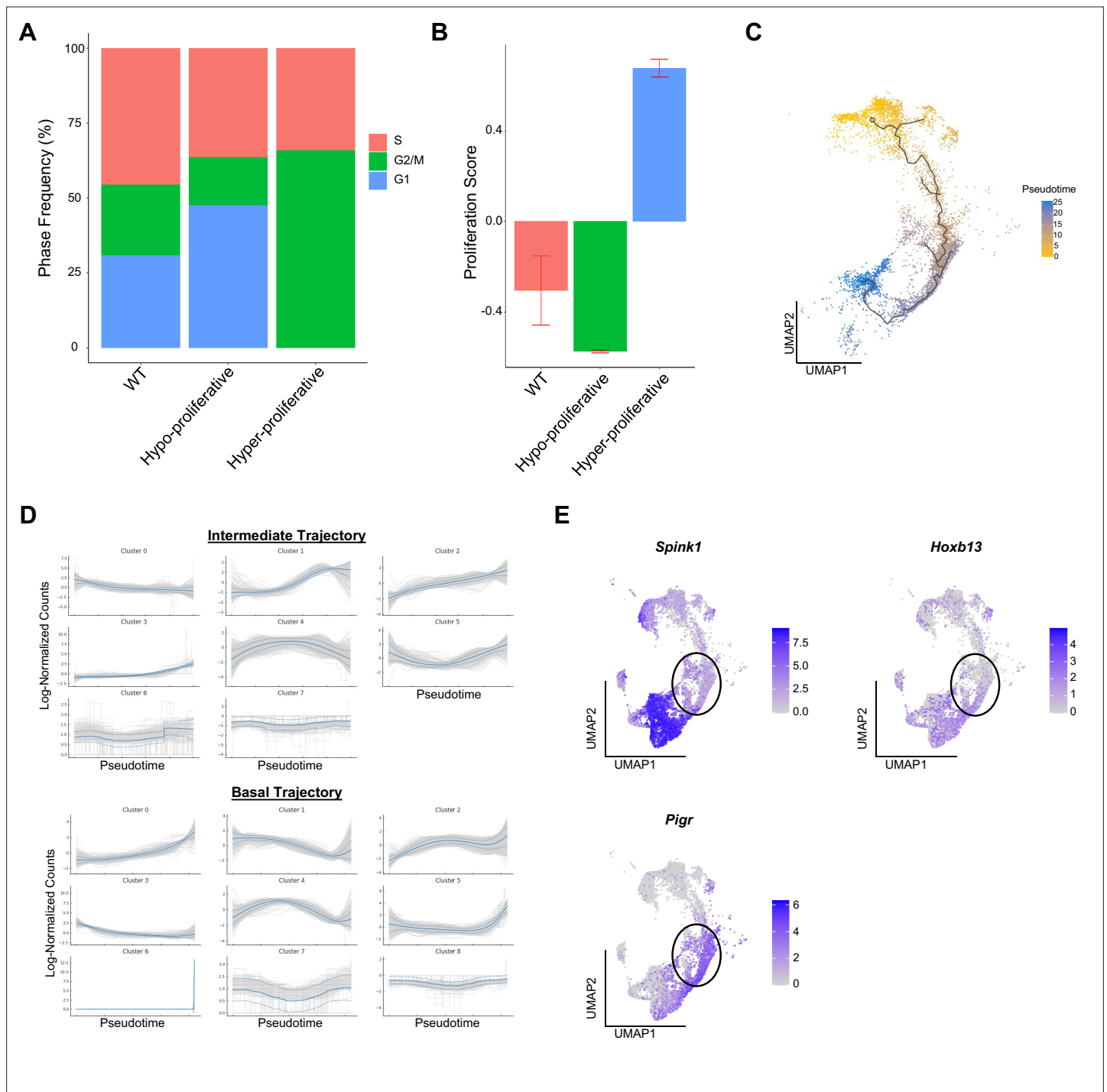


Figure 1—figure supplement 2. Basal proliferation is subset-specific and intermediate cells express luminal markers. **(A)** Bar plot of cell cycle phase assignments in WT basal cells and *Pten^{fl/fl}* hyper- and hypo-proliferative basal cells. **(B)** Bar plot of CCP signature composite score in WT (n=3) basal cells and *Pten^{fl/fl}* (n=2) hyper- and hypo-proliferative basal cells (Data presented as \pm SD). **(C)** Trajectory analysis of *Pten^{fl/fl}* epithelial cells. **(D)** Top 3000 highly variable genes in *Pten^{fl/fl}* basal and intermediate cells, clustered by expression pattern along the basal-intermediate (top) or hypo-proliferative basal-hyper-proliferative basal (bottom) trajectories drawn via Palantir (**Figure 1I**). **(E)** UMAP visualization of luminal biomarkers in epithelial cells in WT and *Pten^{fl/fl}* mice. Black circles indicate luminal-intermediate transition zone.

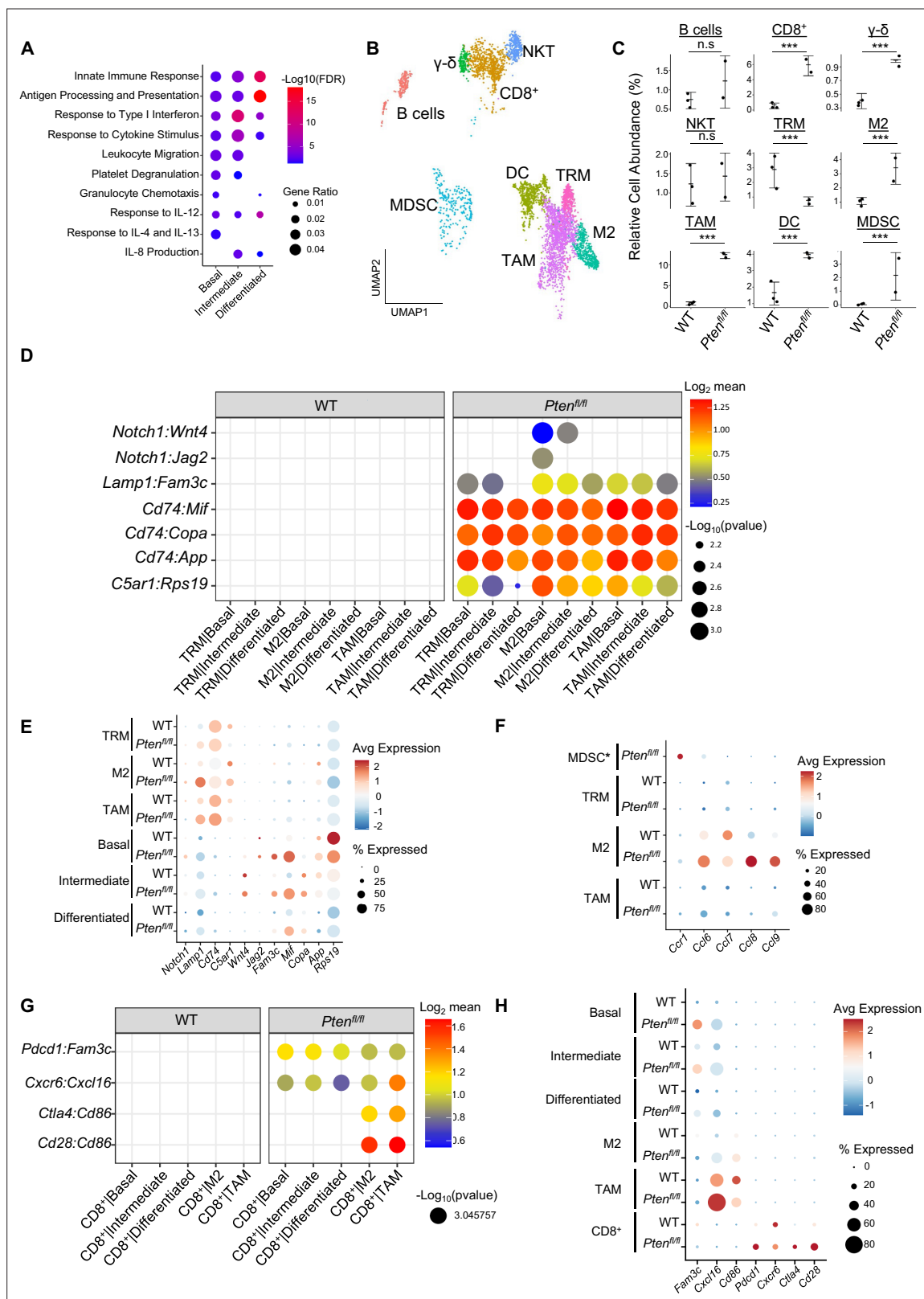


Figure 2. Immune recruitment in *Pten*^{fl/fl} prostates is mediated by both epithelial and immune cell signaling. **(A)** Top immune-related GSEA results enriched in *Pten*^{fl/fl} compared to WT mice for each epithelial subtype. All pathways are enriched with FDR <0.05. **(B)** UMAP visualization of immune cells labeled by cell subtype or state. **(C)** Relative abundance of immune cells in WT (n=3) and *Pten*^{fl/fl} (n=2) mice. Y-axis shows the % composition of each sample by cell type (Data presented as +/SD, ***p<0.001, n.s.=not significant, negative binomial test). **(D)** Dot plot of signaling interactions between

Figure 2 continued on next page

Figure 2 continued

macrophages and epithelial cells. Y-axis, ligand-receptor pairs from CellphoneDB database. X-axis, cell-cell pairings. Interactions are directional: the first gene in a pair is expressed in the first cell in the cell-cell interaction. **(E)** Dot plot of epithelial ligand and macrophage receptor gene expression in WT and *Pten^{fl/fl}* mice. **(F)** Dot plot of *Ccr1* and *Ccr1* ligand expression in MDSCs and macrophages in WT and *Pten^{fl/fl}* ventral prostates. MDSCs are only present in *Pten^{fl/fl}* and therefore do not have a WT row (denoted by asterisk). **(G)** Plot of signaling interactions between CD8⁺ T cells and epithelial cells and macrophages. **(H)** Dot plot of CD8⁺ T cell receptors and epithelial and macrophage ligand gene expression in WT and *Pten^{fl/fl}* ventral prostates.

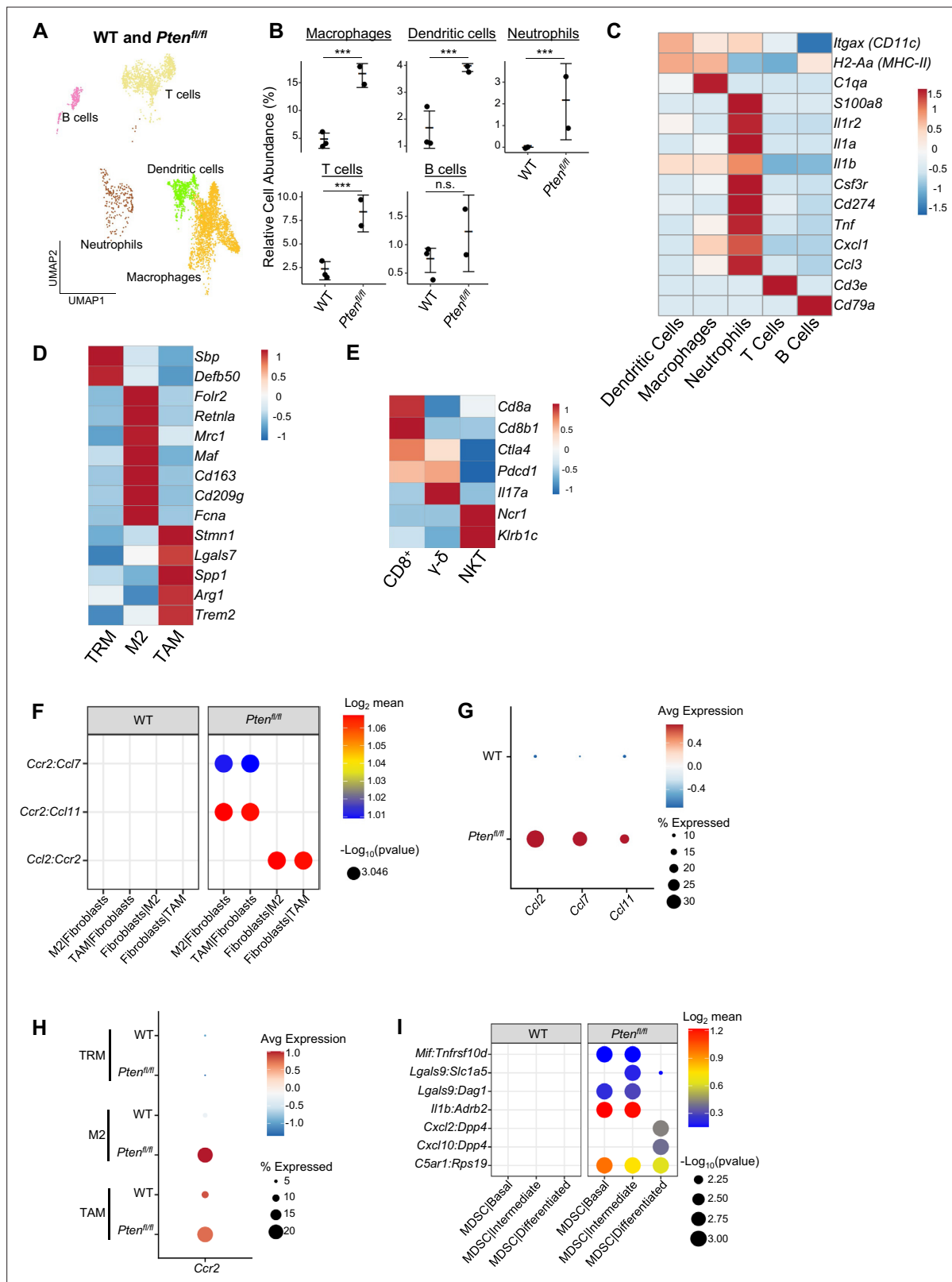


Figure 2—figure supplement 1. Immune cells contain pro-tumorigenic subtypes and macrophages are recruited by fibroblast signaling. (A) UMAP of immune cells in WT and *Pten^{fl/fl}* prostates, labeled by cell types. (B) Relative abundance of immune cell types in WT (n=3) and *Pten^{fl/fl}* (n=2) mice (***p<0.001, n.s.=not significant, negative binomial regression test). (C) Heatmap of immune cell type biomarker expression in WT and *Pten^{fl/fl}* mice; neutrophil cells express MDSC markers. Log-transformed read counts. (D) Heatmap of marker expression in macrophage cell subtypes. Log-transformed read counts. Figure 2—figure supplement 1 continued on next page

Figure 2—figure supplement 1 continued

read counts. **(E)** Heatmap of marker expression in T cell subtypes. Log-transformed read counts. **(F)** Plot of ligand-receptor interactions between fibroblast and macrophage subtypes. **(G)** Dot plot of *Ccr2* ligand expression in fibroblasts in WT and *Pten^{fl/fl}* ventral prostates. **(H)** Dot plot of *Ccr2* expression in macrophage subtypes in WT and *Pten^{fl/fl}* ventral prostates. **(I)** Dot plot of signaling interactions between epithelial cells and MDSCs.

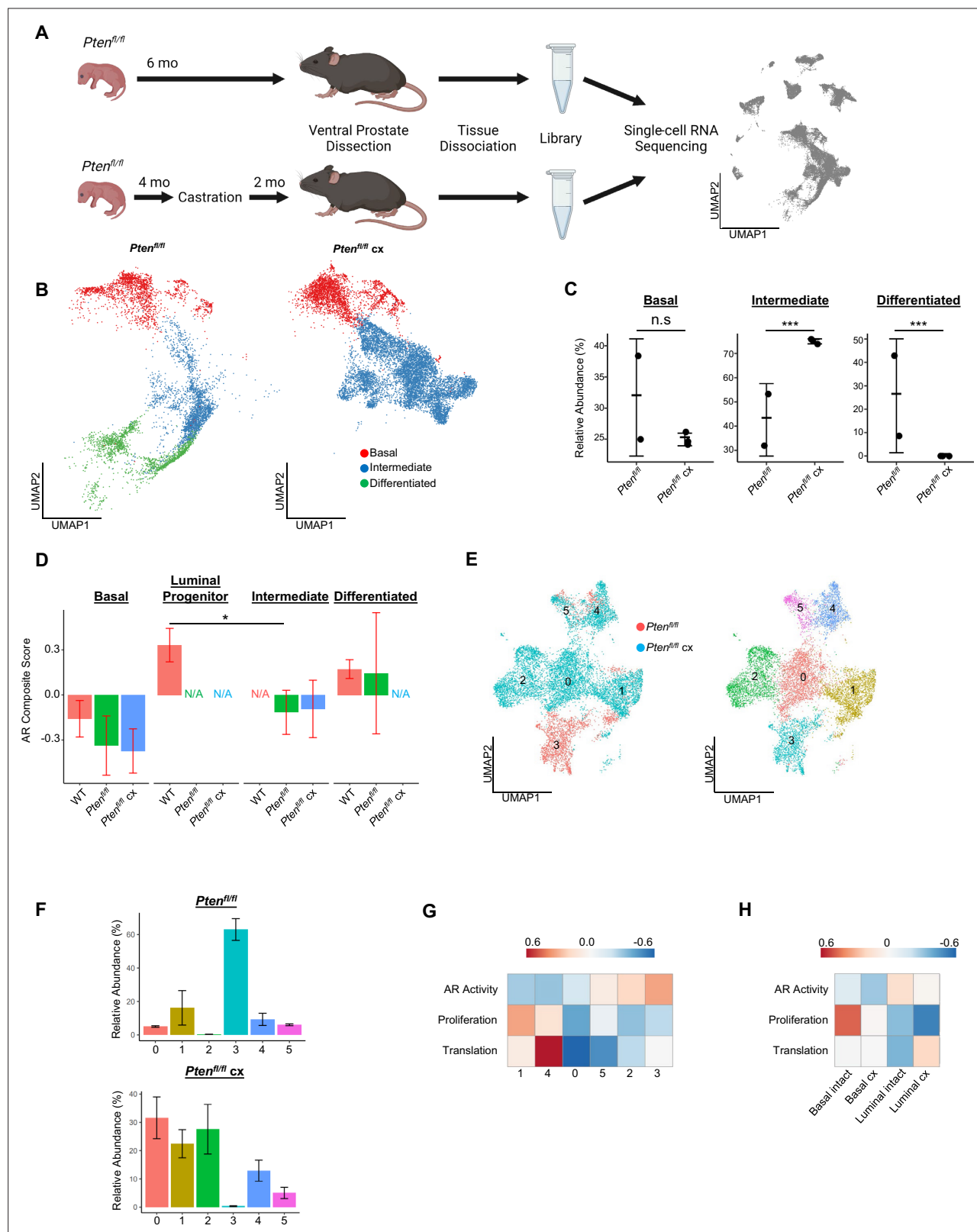


Figure 3. Intermediate cells are primed for survival and diversification in the context of castration. **(A)** Simplified schematic of setup for single-cell sequencing of *Pten^{fl/fl}* intact and *Pten^{fl/fl}* castrated (cx) ventral prostates. **(B)** Split UMAP visualizations of *Pten^{fl/fl}* and *Pten^{fl/fl} cx* epithelial cells. **(C)** Relative abundance of epithelial cells in *Pten^{fl/fl}* intact (n=2) and *Pten^{fl/fl} cx* (n=3) prostates. Y-axis shows the % composition of each sample by cell type (Data presented as \pm SD, ***p<0.001, n.s.=not significant, negative binomial test). **(D)** Androgen Receptor (AR) gene signature composite score in epithelial cells, Figure 3 continued on next page

Figure 3 continued

clustered by condition (Data presented as \pm -SD, $*p < 0.05$, permutation test). N/A indicates missing data due to no cells being present in the condition. WT $n=3$, *Pten*^{fl/fl} intact $n=2$, *Pten*^{fl/fl} cx $n=3$. **(E)** UMAP visualization of intermediate cells in *Pten*^{fl/fl} intact and cx prostates. Left, colored by condition; right, colored by clusters 0–5. **(F)** Relative abundance of intermediate clusters. Top, intact *Pten*^{fl/fl} ($n=2$); bottom, *Pten*^{fl/fl} cx ($n=3$) (Data presented as \pm -SD). **(G)** Heatmap of composite score for AR, CCP, and Reactome translation gene signatures in intermediate clusters. **(H)** Heatmap of composite score for AR, CCP, and Reactome translation gene signatures in WT intact and castrate basal and luminal cells.

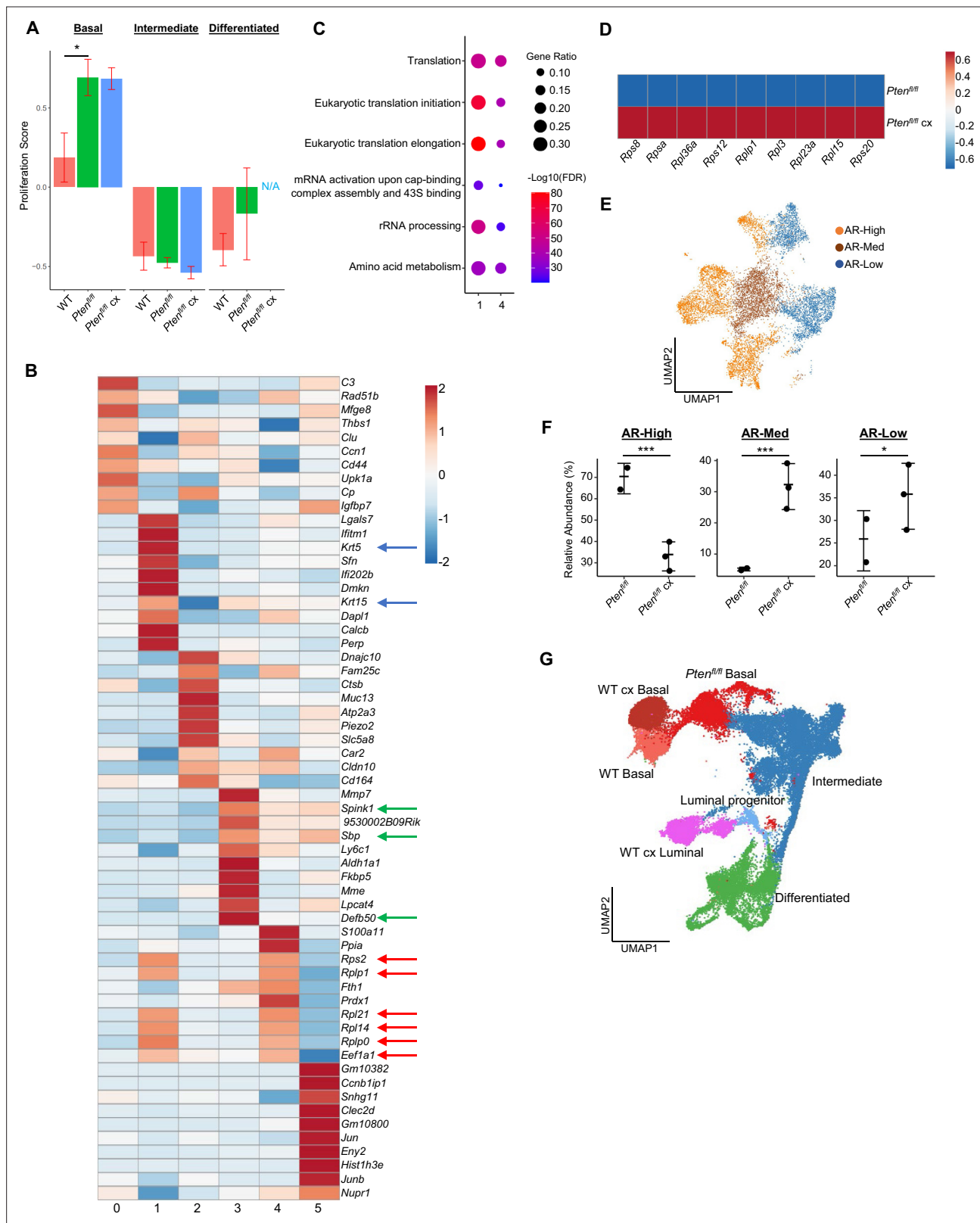
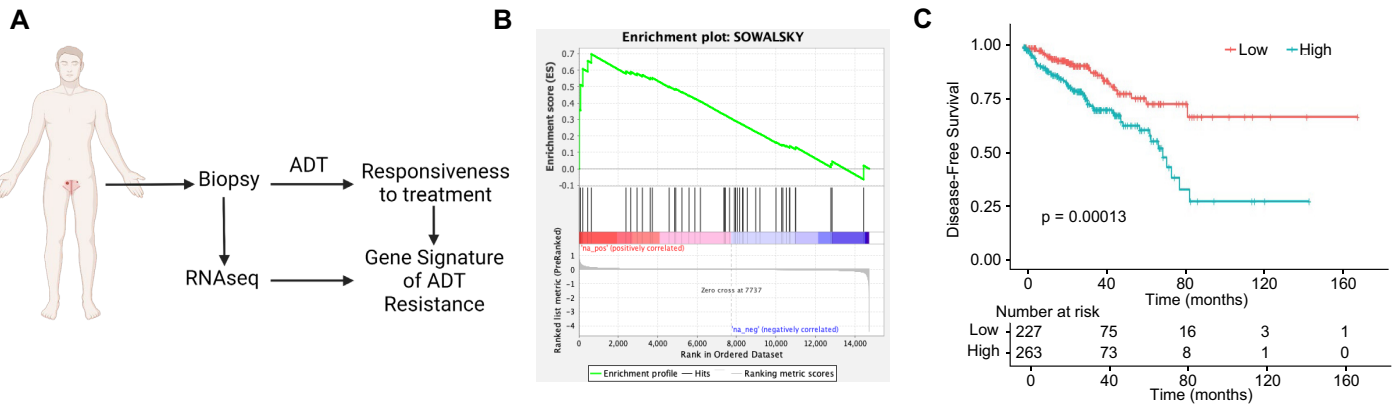


Figure 3—figure supplement 1. Castration-resistant intermediate cells are phenotypically diverse. (A) Composite score of CCP signature in WT, *Pten^{fl/fl}* intact, and *Pten^{fl/fl} cx* epithelial cells (Data presented as +/-SD, *p<0.05, permutation test) (B) Heatmap of top differentially expressed genes across intermediate clusters 0-5. Blue arrows, basal markers; green arrows, AR-dependent genes; red arrows, ribosomal or translation machinery genes. (C) Top GSEA results for genes upregulated in intermediate clusters 1 and 4. All pathways are enriched with FDR <0.05. (D) Heatmap of ribosomal gene expression. Figure 3—figure supplement 1 continued on next page

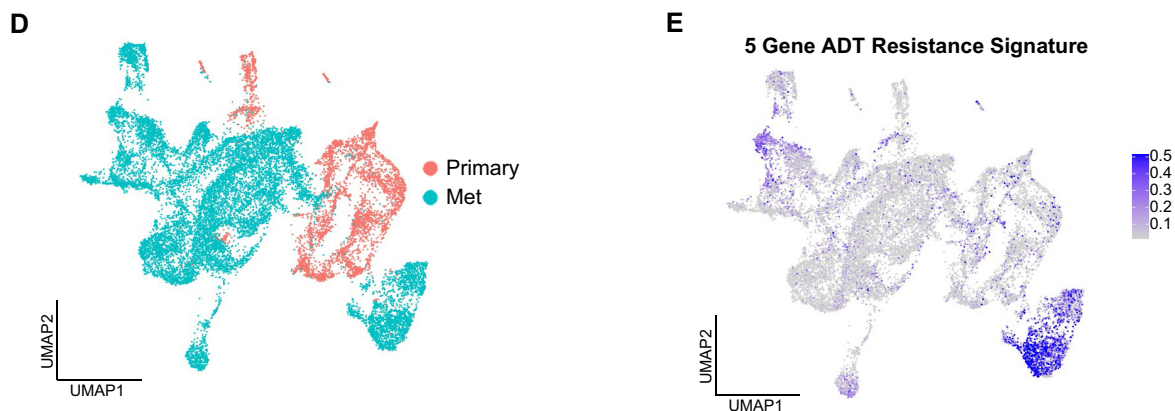
Figure 3—figure supplement 1 continued

expression in basal cells in *Pten^{fl/fl}* intact and *Pten^{fl/fl}* cx mice. **(E)** UMAP visualization of AR signaling status in intermediate cells in *Pten^{fl/fl}* intact and *Pten^{fl/fl}* cx mice. **(F)** Relative abundance of intermediate cells with high, medium, or low AR signaling in *Pten^{fl/fl}* intact (n=2) and *Pten^{fl/fl}* cx (n=3) mice (Data presented as +/-SD, *p<0.05, ***p<0.001, negative binomial regression test). **(G)** UMAP visualization of epithelial cells in WT intact, WT cx, *Pten^{fl/fl}* intact, and *Pten^{fl/fl}* cx mice, colored and labeled by cell ID.

Intermediate-Derived Signature Correlates with Poor Prognosis in Human Patients



scRNAseq of Patient Samples Shows Enriched Intermediate Signature in Metastasis



ADT Resistance Signature Correlates with Castration Resistance in Orthogonal Model

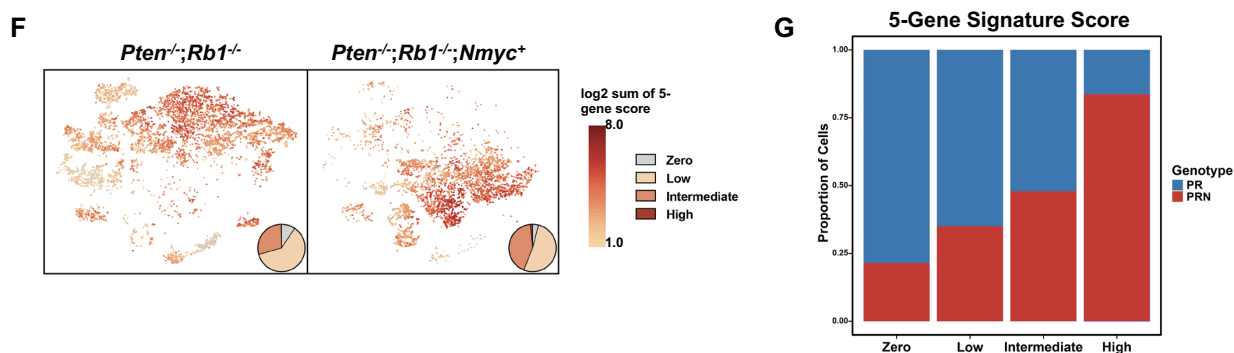


Figure 4. Intermediate cells are enriched for a signature of treatment resistance that correlates with advanced human disease. (A) Diagram of clinical trial used to establish gene signature of androgen deprivation treatment resistance (NCT02430480). (B) Enrichment plot of ADT resistance gene signature relative to intermediate cell DEGs between *Pten*^{fl/fl} and *Pten*^{fl/fl} cx (adjusted p-value = 0.00381). (C) Kaplan-Meier curve of disease-free survival for prostate cancer patients in TCGA database with or without high RNA expression of top correlated genes from B. Red line, patients with normal expression of all genes; blue line, patients with expression of at least 1 gene with TPM (transcripts per million) in the 80th percentile or above. (D) UMAP of tumor cells from human patient samples. Red, primary cancer; blue, metastatic cancer. (E) UMAP visualization of per-cell computed score for 5-gene signature from (B-C) in human cancer samples. (F) UMAP visualization of per-cell computed score for 5-gene signature from (B-C) in PR and PRN mouse

Figure 4 continued on next page

Figure 4 continued

models. Pie charts indicate proportion of cells with zero, low, intermediate, or high signature scores. **(G)** Stacked bar chart showing proportion of cells from PR or PRN mice in each scoring category for the 5-gene signature.

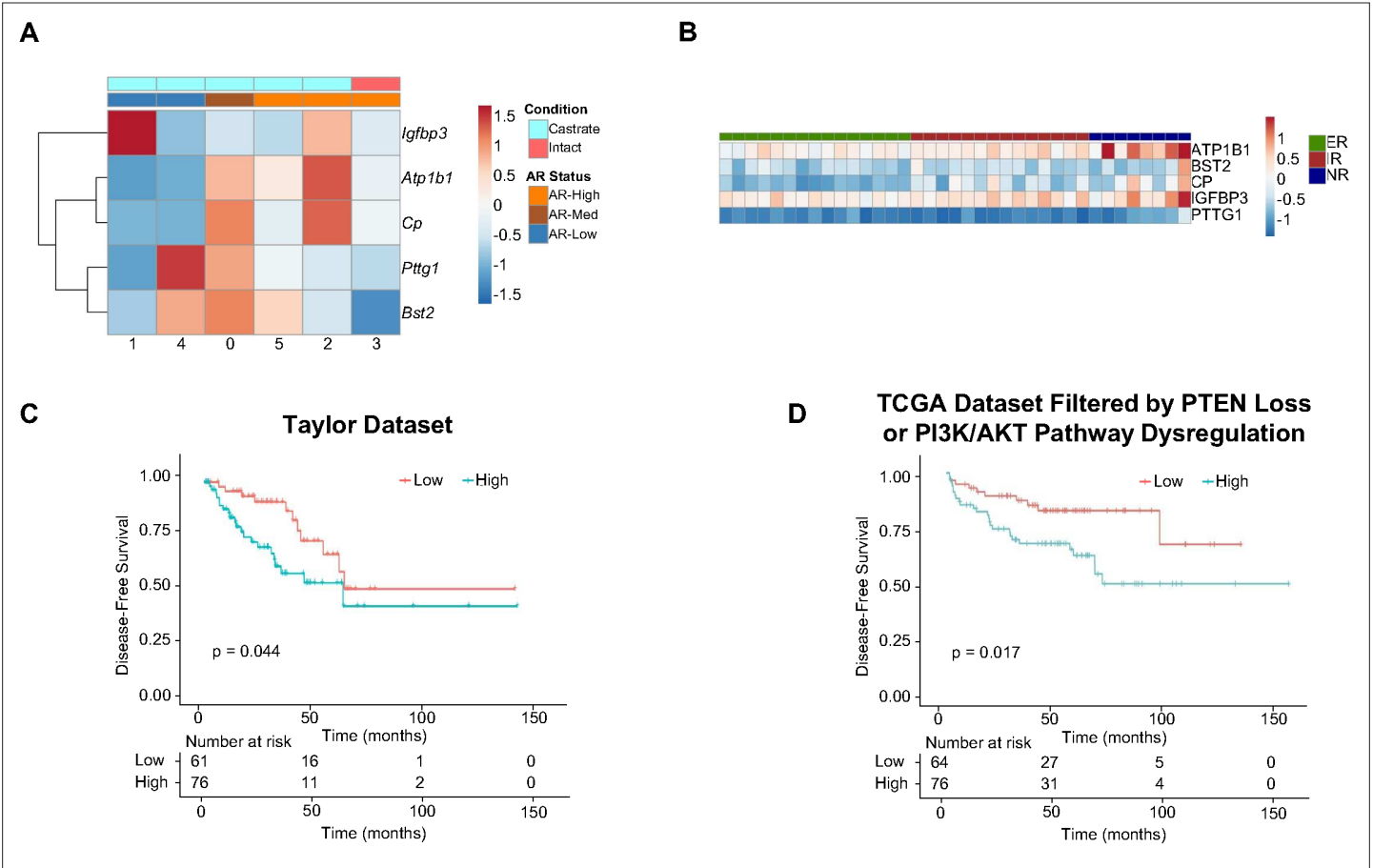


Figure 4—figure supplement 1. 5 Genes expressed in intermediate cells correlate with poor disease outcomes in human patients. **(A)** Heatmap of top 5 resistance genes in intermediate clusters, labeled by AR status and condition (intact or castrate). **(B)** Heatmap of the top 5 genes enriched in castrated intermediate cells (**Figure 4B**) and their expression in ADT non-responder (NR), intermediate responder (IR), and excellent responder (ER) patients. **(C)** Kaplan-Meier curve of disease-free survival of patients in the Taylor et al., 2010 cohort, separated by expression of the top 5 resistance genes in castrated intermediate cells. Red line, normal expression of top 5 genes; blue line, patients with expression of at least 1 gene with TPM in the 80th percentile or above. **(D)** Kaplan-Meier curve of disease-free survival of patients in the TCGA database, filtered for PTEN loss or PI3K/AKT pathway dysregulation, separated by expression of the top 5 resistance genes in castrated intermediate cells. Red line, normal expression of top 5 genes; blue line, patients with expression of at least 1 gene with TPM (transcripts per million) in the 80th percentile or above.

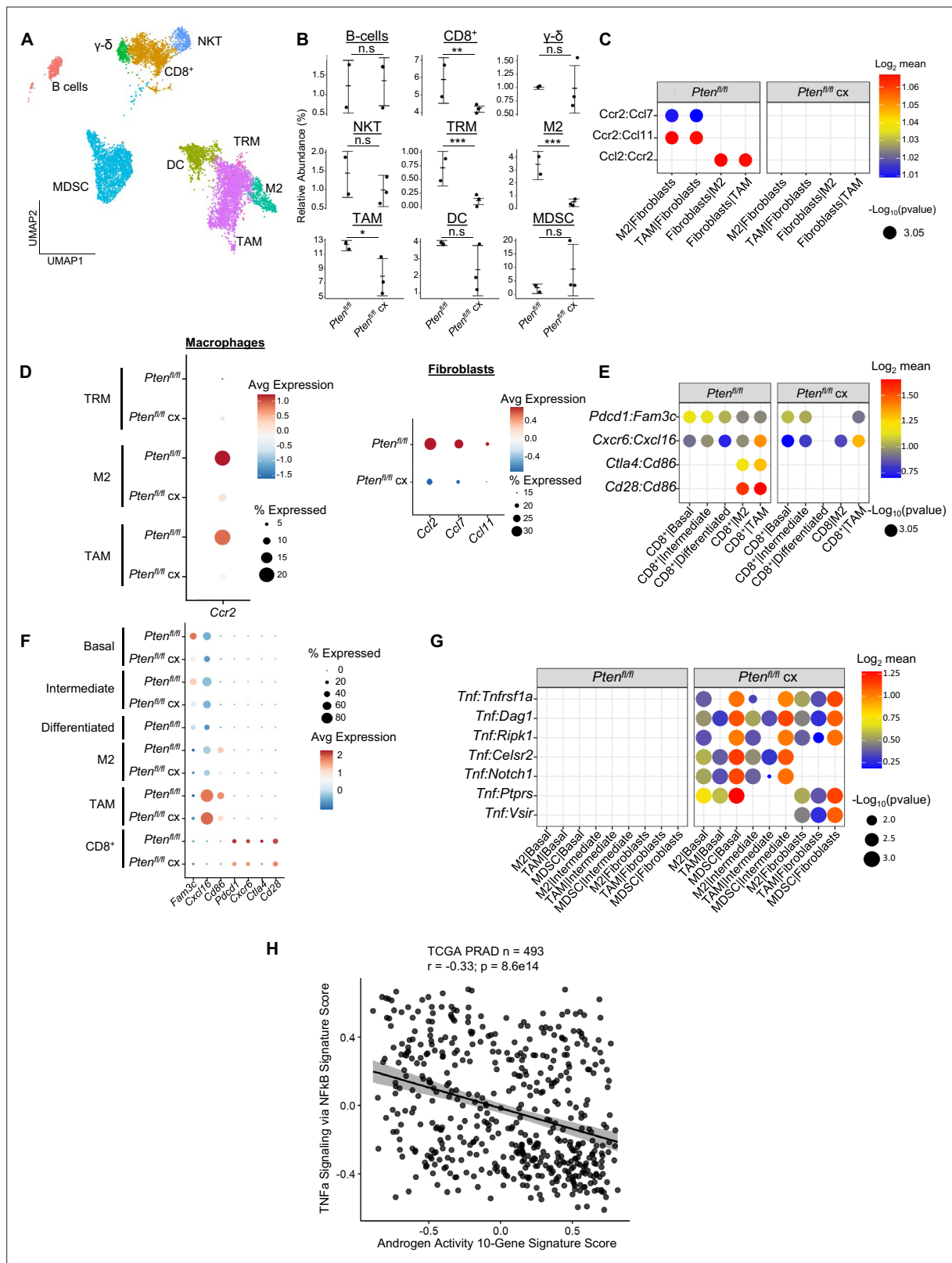


Figure 5. Castration remodels immune environment via fibroblast signaling and increases TNF pathway activity. **(A)** Combined UMAP visualization of immune cells in *Pten^{fl/fl}* and *Pten^{fl/fl} cx* ventral prostates. **(B)** Relative abundance of immune cells in *Pten^{fl/fl}* intact (n=2) and *Pten^{fl/fl} cx* (n=3) mice. Y-axis shows the % composition of each sample by cell type (Data presented as \pm SD, * $p < 0.05$, ** $p < 0.01$, *** $p < 0.001$, n.s.=not significant, negative binomial test). **(C)** Dot plot of signaling interactions between macrophages and fibroblasts. **(D)** Dot plot of *Ccr2* expression in M2 macrophages and TAMs (left). Dot plot of *Ccr2* expression in M2 macrophages and TAMs (right). **(E)** Dot plot of *Ccr2* expression in M2 macrophages and TAMs (left). Dot plot of *Ccr2* expression in M2 macrophages and TAMs (right). **(F)** Dot plot of *Ccr2* expression in M2 macrophages and TAMs (left). Dot plot of *Ccr2* expression in M2 macrophages and TAMs (right). **(G)** Dot plot of *Ccr2* expression in M2 macrophages and TAMs (left). Dot plot of *Ccr2* expression in M2 macrophages and TAMs (right). **(H)** Scatter plot showing the correlation between TNF α Signaling via NFkB Signature Score and Androgen Activity 10-Genes Signature Score. TCGA PRAD n = 493, $r = -0.33$; $p = 8.6e14$.

Figure 5 continued

of *Ccr2* ligand expression in fibroblasts in *Pten^{fl/fl}* intact and cx mice (right). **(E)** Dot plot of signaling interactions between CD8⁺ T cells and epithelial and macrophage cells in *Pten^{fl/fl}* intact and cx mice. **(F)** Dot plot of epithelial and macrophage ligands and CD8⁺ T cell receptor gene expression in *Pten^{fl/fl}* intact and cx mice. **(G)** Dot plot of *Tnf* signaling interactions between myeloid and epithelial/fibroblast cells in *Pten^{fl/fl}* intact and cx prostates. **(H)** Scatter plot of TCGA PRAD study patient signature composite scores. Y-axis, TNF signaling signature score; X-axis, AR signaling signature score (Pearson's correlation).

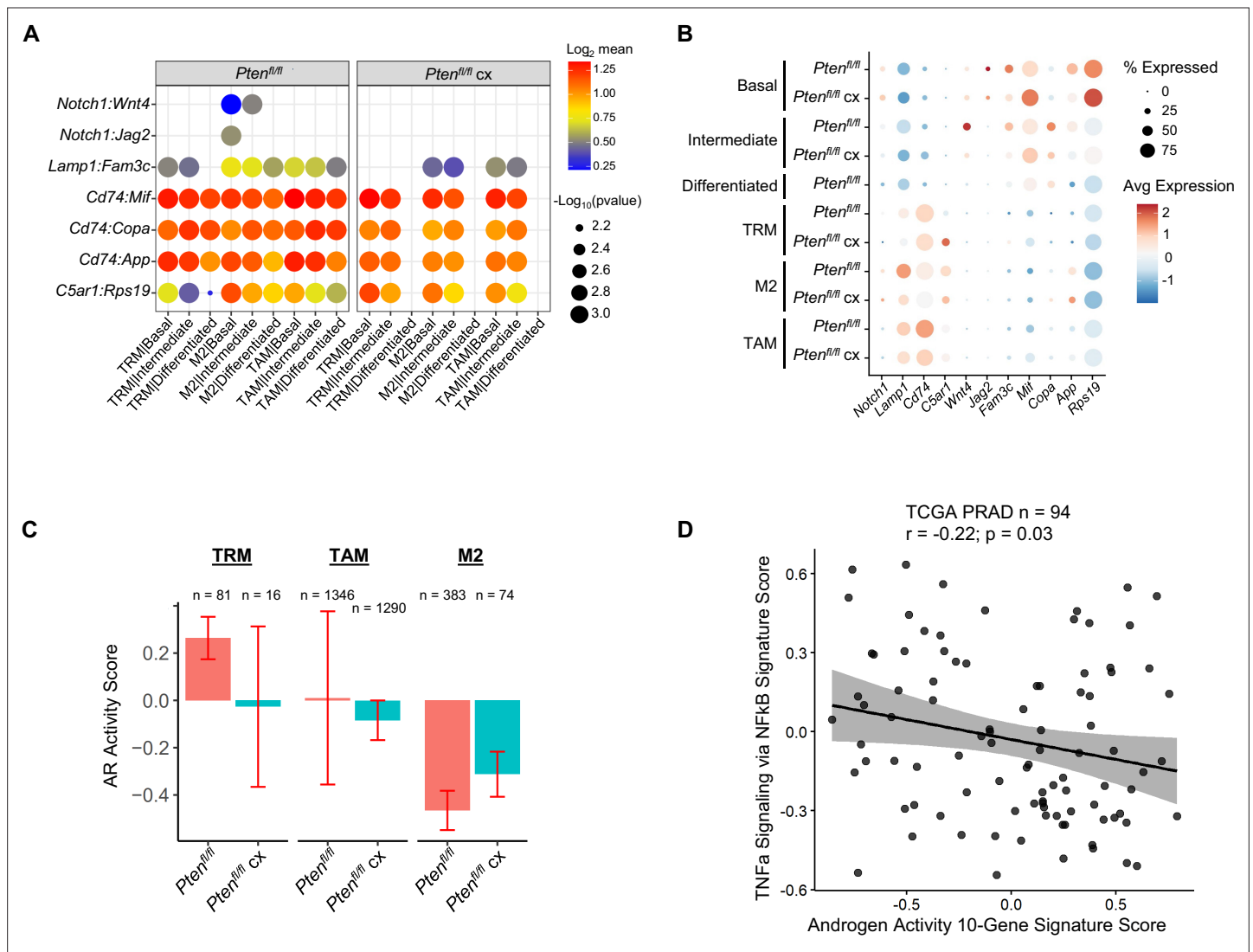


Figure 5—figure supplement 1. Epithelial-mediated macrophage recruitment is not interrupted by castration. **(A)** Plot of signaling interactions between macrophage subtypes and epithelial cells in *Pten^{fl/fl}* intact and *Pten^{fl/fl} cx* prostates. **(B)** Dot plot of epithelial ligand and macrophage receptor gene expression in *Pten^{fl/fl}* intact and *Pten^{fl/fl} cx* ventral prostates. **(C)** Composite score of AR signaling signature in macrophage subtypes in *Pten^{fl/fl}* intact and *Pten^{fl/fl} cx* prostates (Data presented as \pm SD). **(D)** Scatter plot of TCGA PRAD study patient signature composite scores, filtered for patients harboring PTEN mutations. Y-axis, TNF signaling signature score; X-axis, AR signaling signature score (Pearson's correlation).

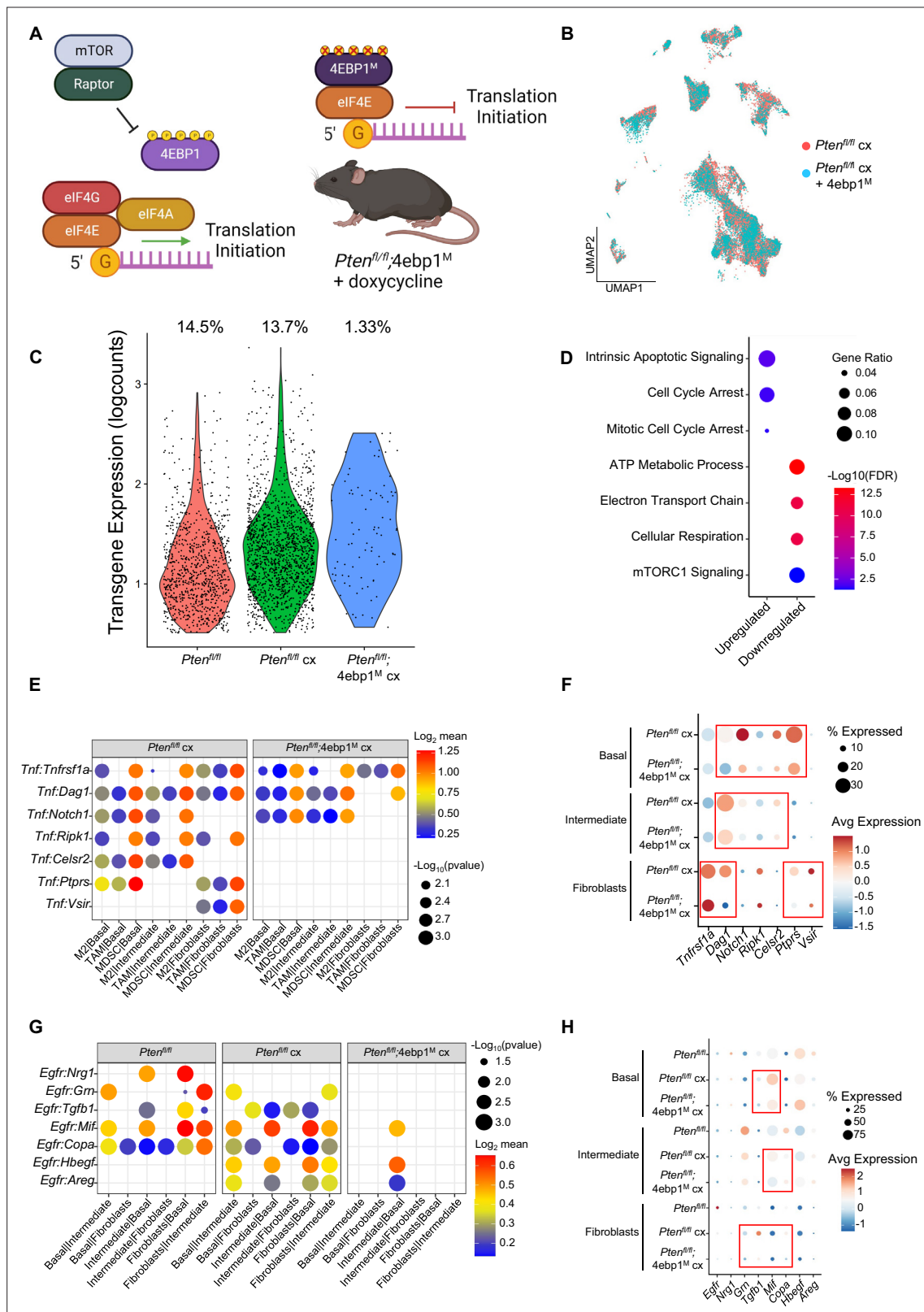


Figure 6. 4EBP1^M expression is lethal in epithelial cells and decreases EGFR and TNF ligands in epithelial cells and fibroblasts. (A) Simplified schematic of the eIF4F translation initiation complex and how the 4EBP1^M protein functions in the *Pten^{fl/fl};4ebp1^M* mouse model when treated with doxycycline.

(B) UMAP visualization of epithelial cells in *Pten^{fl/fl}* cx and *Pten^{fl/fl};4ebp1^M* cx prostates, colored by genotype. (C) Violin plot of *rtTA-eGFP* transgene expression in epithelial cells in each *Pten^{fl/fl}* condition. Plot shows only cells expressing the transgene; each dot represents a cell. Percentages represent

Figure 6 continued on next page

Figure 6 continued

the proportion of transgene-positive cells in each condition. **(D)** Dot plot of top GSEA results from DEG analysis of transgene-positive basal cells in *Pten^{fl/fl};4ebp1^M* cx mice compared to *Pten^{fl/fl}* cx ventral prostates. All pathways are enriched with FDR <0.05. **(E)** Dot plot of *Tnf* signaling interactions between myeloid and epithelial/fibroblast cells in *Pten^{fl/fl}* cx and *Pten^{fl/fl};4ebp1^M* cx mice. **(F)** Dot plot of *Tnf* and *Tnf* ligand expression in myeloid cells, epithelial cells, and fibroblasts in *Pten^{fl/fl}* cx and *Pten^{fl/fl};4ebp1^M* cx prostates. Red boxes highlight ligands with decreased expression in *Pten^{fl/fl};4ebp1^M* cx mice. **(G)** Plot of *Egfr* signaling interactions between epithelial cells and fibroblasts in *Pten^{fl/fl}* intact, *Pten^{fl/fl}* cx, and *Pten^{fl/fl};4ebp1^M* cx prostates. **(H)** Dot plot of *Egfr* and *Egfr* ligand expression in epithelial cells and fibroblasts in *Pten^{fl/fl}* intact, *Pten^{fl/fl}* cx, and *Pten^{fl/fl};4ebp1^M* cx ventral prostates. Red boxes highlight ligands with decreased expression in *Pten^{fl/fl};4ebp1^M* cx mice.



Figure 6—figure supplement 1. Interactive Portal, Enabling Gene- and Cell- Specific Comparisons Across the Spectrum of Prostate Cancer Initiation and Progression in vivo. Interactive website can be found at <https://atlas.fredhutch.org/hsieh-prostate/>.